Mechanism of Gold Metal Ion Reduction, Nanoparticle Growth and Size Control in Aqueous Amphiphilic Block Copolymer Solutions at Ambient Conditions

Toshio Sakai and Paschalis Alexandridis*

Department of Chemical and Biological Engineering, University at Buffalo, The State University of New York, Buffalo, New York 14260-4200

Received: August 21, 2004; In Final Form: January 31, 2005

Spontaneous formation and efficient stabilization of gold nanoparticles with an average diameter of 7∼20 nm from hydrogen tetrachloroaureate(III) hydrate ($HAuCl_4 \cdot 3H_2O$) were achieved in air-saturated aqueous poly(ethylene oxide)−poly(propylene oxide)−poly(ethylene oxide) (PEO−PPO−PEO) block copolymer solutions at ambient temperature in the absence of any other reducing agent. The particle formation mechanism is considered here on the basis of the block copolymer concentration dependence of absorption spectra, the time dependence (kinetics) of $AuCl_4^-$ reduction, and the block copolymer concentration dependence of particle size. The effects of block copolymer characteristics such as molecular weight (MW), PEO block length, PPO block length, and critical micelle concentration (cmc) are explored by examining several PEO−PPO−PEO block copolymers. Our observations suggest that the formation of gold nanoparticles from $AuCl_4^-$ comprises three main steps: (1) reduction of metal ions by block copolymer in solution, (2) absorption of block copolymer on gold clusters and reduction of metal ions on the surface of these gold clusters, and (3) growth of metal particles stabilized by block copolymers. While both PEO and PPO blocks contribute to the $AuCl_4^-$ reduction (step 1), the PEO contribution appears to be dominant. In step 2, the adsorption of block copolymers on the surface of gold clusters takes place because of the amphiphilic character of the block copolymer (hydrophobicity of PPO). The much higher efficiency of particle formation attained in the PEO−PPO−PEO block copolymer systems as compared to PEO homopolymer systems can be attributed to the adsorption and growth processes (steps 2 and 3) facilitated by the block copolymers. The size of the gold nanoparticles produced is dictated by the above mechanism; the size increases with increasing reaction activity induced by the block copolymer overall molecular weight and is limited by adsorption due to the amphiphilic character of the block copolymers.

Introduction

Poly(ethylene oxide)−poly(propylene oxide)−poly(ethylene oxide) (PEO−PPO−PEO) block copolymers are well-known as dispersion stabilizers,[1,2] pharmaceutical ingredients,[3−5] biomedical materials,[6,7] and templates for the synthesis of mesoporous materials and nanoparticles.[8−13] Variation of the PEO−PPO−PEO block copolymer molecular characteristics, concentration, and temperature allows for unique tunability of block copolymer self-assembly in the presence of selective solvents such as water.[14,15] We have recently found that PEO−PPO−PEO block copolymers can act as very efficient reductants/stabilizers in the single-step synthesis and stabilization of gold nanoparticles from hydrogen tetrachloroaureate(III) hydrate ($HAuCl_4 \cdot 3H_2O$) in air-saturated aqueous solutions at ambient temperature in the absence of additional reductant or energy input.[16,17] This synthesis proceeds fast to completion (in less than 2 h) and is environmentally benign and economical since it involves only water and nontoxic commercially available polymers (Poloxamers or Pluronics).[16,17] The gold nanoparticle dispersions remain highly stable for several months. On the contrary, PEO homopolymer, of molecular weight comparable to that of the PEO−PPO−PEO block copolymers we have considered, was very slow in producing particles (more than 2 days was needed) and inadequate for their colloidal stabilization.[16,17] Compared to recently reported single-step methods for gold nanoparticle synthesis,[18−21] our method offers the advantages of ambient conditions, fast completion, being economical, and resulting in a "ready-to-use" product. To realize the full potential of our approach (and to be able to generalize to other systems) we need better insight into the relationship between particle formation and block copolymer characteristics.

To this end, in the present work we examine the factors that contribute to the reduction of metal ions, particle formation (growth), size control, and colloidal stability in this single-step synthesis of gold nanoparticles in aqueous PEO−PPO−PEO block copolymer solutions. The contributions of block copolymer molar concentration, PEO concentration, PPO concentration, and critical micelle concentration (cmc) are addressed by examining a range of PEO−PPO−PEO block copolymers. Investigations, like the one reported here, of polymer molecular characteristics on the formation of colloidal particles are scarce.[22,23] Polymer effects on the formation of gold nanoparticles have been reported in organic media with polystyrene−poly(4-vinylpyridine) (PS-*b*-P4VP) having various PS and P4VP block lengths.[24] In aqueous systems, the effects of metal ion/stabilizer mixing ratio, reaction temperature, reaction time, and energy input on the formation of colloidal particles typically have been considered.[22,23] The observations we report here suggest that the formation of gold nanoparticles from $AuCl_4^-$ comprises three main steps: (1) reduction of metal ions facilitated by block copolymers in solution, (2) absorption of block copolymers on gold clusters and reduction of metal ions

* To whom correspondence should be addressed: phone (716) 645-2911, ext. 2210; fax (716) 645-3822; e-mail palexand@eng.buffalo.edu.

10.1021/jp046221z CCC: $30.25
Published on Web 03/31/2005

TABLE 1: Properties of the PEO−PPO−PEO Block Copolymers Used in This Study[25]

Pluronic	molecular weight	PEO, wt %	PPO block mol wt	PEO block mol wt	cmc,[a] mM (25 °C)	nominal formula
L43	1850	30	1295	555		$EO_6PO_{22}EO_6$
L44	2200	40	1320	880		$EO_{10}PO_{23}EO_{10}$
L62	2500	20	2000	500		$EO_6PO_{34}EO_6$
L64	2900	40	1740	1160	26.31	$EO_{13}PO_{30}EO_{13}$
P65	3400	50	1700	1700	38.22	$EO_{19}PO_{29}EO_{19}$
F68	8400	80	1680	6720	320.5	$EO_{76}PO_{29}EO_{76}$
P84	4200	40	2520	1680	6.190	$EO_{19}PO_{43}EO_{19}$
P85	4600	50	2300	2300	8.695	$EO_{26}PO_{40}EO_{26}$
F88	11 400	80	2280	9120	11.51	$EO_{103}PO_{39}EO_{103}$
P103	4950	30	3465	1485	0.141	$EO_{17}PO_{60}EO_{17}$
P104	5900	40	3540	2360	0.508	$EO_{27}PO_{61}EO_{27}$
P105	6500	50	3250	3250	0.461	$EO_{37}PO_{56}EO_{37}$
F108	14 600	80	2920	11680	3.082	$EO_{132}PO_{50}EO_{132}$
P123	5750	30	4025	1725	0.052	$EO_{19}PO_{69}EO_{19}$
F127	12 600	70	3780	8820	0.555	$EO_{100}PO_{65}EO_{100}$
PEO	6000	100	0	6000		EO_{136}

[a] Critical micelle concentration.

on the surface of these gold clusters, and (3) growth of gold particles and stabilization by block copolymers. The final condition (the result of steps 1−3) is examined by analysis of the absorption spectra recorded after the reaction completion. The initial reduction process (step 1) is identified by kinetics data obtained at the early stages of $AuCl_4^-$ reduction. The particle growth process (steps 2 and 3) is discussed by particle size determination by electron microscopy. The sizes observed support our proposed mechanism for particle growth. Moreover, comparison of various PEO−PPO−PEO block copolymers reveals that the overall block copolymer (i.e., both PEO and PPO blocks) contributes to $AuCl_4^-$ reduction and particle formation. PEO is more dominant than PPO in the initial stages of reduction. PPO facilitates block copolymer adsorption on gold clusters and reduction of $AuCl_4^-$ ions on the surface of these gold clusters and/or particles. The difference in particle formation observed between PEO−PPO−PEO block copolymer systems and PEO homopolymer systems is attributed to the block copolymer adsorption and $AuCl_4^-$ reduction processes on the surface of gold clusters and/or particles (steps 2 and 3).

Experimental Section

Synthesis of Gold Nanoparticles. Gold nanoparticles were prepared by simply mixing an aqueous 2×10^{-3} mol L^{-1} hydrogen tetrachloroaureate(III) hydrate ($HAuCl_4 \cdot 3H_2O$; 99.9+ %, Aldrich) solution with an aqueous solution of homopolymer PEO (PEG6000, Fluka Biochemika) or PEO−PPO−PEO block copolymer so that the $AuCl_4^-$ concentration in the reaction medium was 2×10^{-4} mol L^{-1}. The polymer concentrations reported here are those of the aqueous polymer solution prior to mixing with the $HAuCl_4$ solution. The mixing ratio was such that the polymer concentration in the reaction medium was 10% lower than that before mixing. Following agitation by vortex mixer for ~10 s, the solutions were left standing at 25 ± 1 °C for 2 h for the reaction to proceed (note: the absorbance spectra remained almost unchanged after 2 h, indicating completion of the reaction). This reaction takes place under both ambient light and dark conditions. Various PEO−PPO−PEO block copoly-

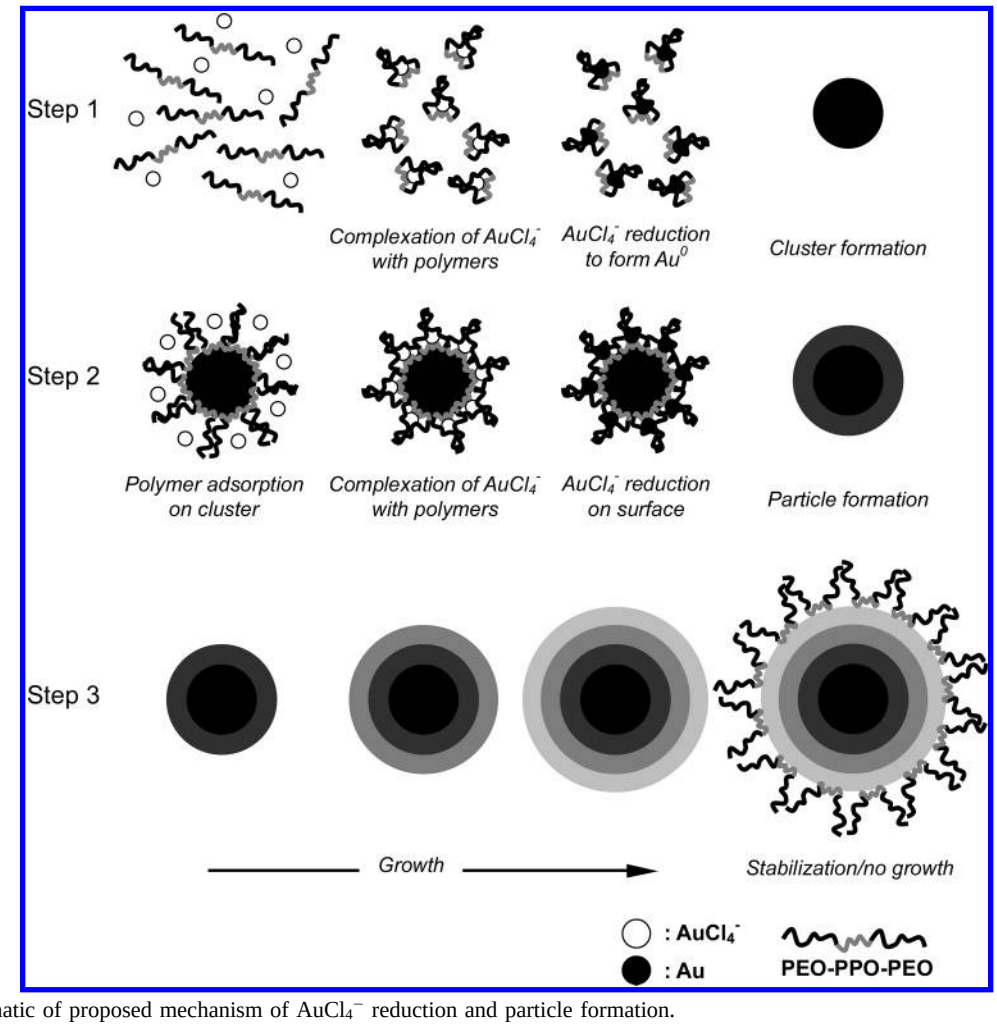

Figure 1. Schematic of proposed mechanism of $AuCl_4^-$ reduction and particle formation.

mers (Pluronic L43, L44, L62, L64, P65, F68, P84, P85, F88, P103, P104, P105, F108, P123, and F127; BASF Corp.) were selected in this study in order to examine the effects of block copolymer molecular weight, PEO block length, PPO block length, PEO/PPO block ratio, and presence of block copolymer micelles on the synthesis of gold nanoparticles. Properties of the PEO−PPO−PEO block copolymers considered here are listed in Table 1.[25]

Characterization. The reduction of $AuCl_4^-$ and the formation of gold nanoparticles were monitored by observing changes in the absorption bands centered at ~220 nm due to the gold(III) chloride ions[26] and those centered at ~540 nm originating from the surface plasmon of the gold nanoparticles[27,28] on a UV−visible spectrometer (Genesys 6, Thermo Spectronic). The wavelength of 240 nm (as opposed to the band maximum that is at ~220 nm) was used to estimate the amount of $AuCl_4^-$ reduced by use of the extinction coefficient value of 9823 M^{-1} cm^{-1} that has been reported at this wavelength.[26] The size and shape of the obtained gold nanoparticles were observed by transmission electron microscopy (JEM-100CX, JEOL Ltd., ×100K) in conventional transmission mode using 80-keV. The particle size distributions were obtained by measuring the diameters of more than 500 particles viewed in the micrographs.

Metal Ion Reduction by PEO−PPO−PEO Block Copolymers. To clarify the mechanism of $AuCl_4^-$ reduction by PEO−PPO−PEO block copolymers, we consider below three possibilities on the basis of information reported for the reduction of metal ions by PEO-type surfactants,[29,30] PEO homopolymer,[18,31−40] and PEO-containing polymers:[13,19,20,32−40]

(a) The alcohol (hydroxyl) functionality at the two ends of a PEO−PPO−PEO block copolymer molecule could act as reductant for the metal ions.[23,29] Alcohols are often used as reductants for the synthesis of metal nanoparticles.[23,29] However, according to our experiments, alcohols (e.g., methanol, ethanol, 1-propanol, 2-propanol, ethylene glycol, and glycerol) at concentrations less than 5 mM (consistent with the PEO−PPO−PEO block copolymer concentration range used in our work) do not lead to observable reduction of $AuCl_4^-$ ions.

(b) Hydroperoxides (ROCOOH) that can be formed by polyethers such as PEO−PPO−PEO block copolymers upon reaction with oxygen from the air[41] have both oxidizing and weakly reducing properties.[13,29,30] Barnickel and Wokaun[29] have reported spontaneous reduction of $AuCl_4^-$ ions in water-in-oil microemulsion systems stabilized by dodecyl hepta(ethylene glycol) ether [$C_{12}H_{25}O(CH_2CH_2O)_6CH_2CH_2OH$]. They proposed that hydroperoxides formed from oxidation of the surfactant[41] most likely were responsible for metal ion reduction. To examine this possible mechanism, we tested the formation of gold nanoparticles with PEO−PPO−PEO block copolymers (e.g., $EO_6PO_{22}EO_6$, Pluronic L44) having PEO block length comparable to that of the reported PEO-type surfactants,[29,30] and found that $AuCl_4^-$ reduction and gold nanoparticle formation were hardly observed. Even if PEO−PPO−PEO block copolymers were forming hydroperoxides in air-saturated water, this effect is significantly small.

(c) The PEO in PEO−PPO−PEO block copolymers forms cavities (pseudo-crown ether structure) that can bind metal ions,[32−40] and reduction of bound $AuCl_4^-$ ions can proceed via oxidation of the oxyethylene and oxypropylene segments by the metal center.[18] PEO is known to form in aqueous solution a conformation similar to crown ethers (pseudo-crown ether structure) that is able to bind with metal ions.[34,35] The induced cyclization is caused by ion−dipole interactions between the templating ion and the electron lone pairs of the ethylene oxide linkages.[32,33] The interaction between metal ions and PEO becomes important for longer (>EO_7) PEO chains.[32,33] Several oxygen atoms in the PEO chain interact with one ion and therefore the strength of the attraction depends on the length of the PEO chain.[32,33,38] Our experimental results, in particular, the effects of block copolymer block length (molecular weight), are consistent with this mechanism. Thus we believe this mechanism to be primarily responsible for metal ion reduction in PEO−PPO−PEO block copolymer systems.

Results and Discussion

Proposed Mechanism of Gold Nanoparticle Formation. Let us first describe the proposed mechanism of $AuCl_4^-$ reduction and particle formation in aqueous PEO−PPO−PEO block copolymer solutions (the results presented in the following sections will be discussed in the context of this proposed mechanism). Our findings indicate that the formation of gold nanoparticles from $AuCl_4^-$ includes three main steps (see Figure 1): (1) reduction of metal ions in solution facilitated by block copolymers to form gold clusters, (2) absorption of block copolymer on the surface of gold clusters and reduction of metal ions in that vicinity, and (3) growth of gold particles and colloidal stabilization by block copolymers.

Step 1: Reduction of Metal Ions in Aqueous PEO−PPO−PEO Block Copolymer Solution. The mechanism of gold ion reduction by PEO−PPO−PEO block copolymers in aqueous solutions is presumed to be the same as that proposed in aqueous PEO homopolymer solutions.[18] The polymers form pseudo-crown ether structures (cavities) with $AuCl_4^-$ ions:

$$AuCl_4^- + n\text{PEO}-\text{PPO}-\text{PEO} \rightarrow (AuCl_4^-)-(\text{PEO}-\text{PPO}-\text{PEO})_n \quad (1)$$

where $(AuCl_4^-)-(PEO-PPO-PEO)_n$ represents $AuCl_4^-$ ions bound to cavities that are formed from hydrated PEO and PPO coils.[33−35] Reduction of bound $AuCl_4^-$ ions proceeds via oxidation of the polymer by the metal center.[18] Oxidation products (carboxylate groups) have been identified by Fourier transform infrared spectroscopy (FT-IR) in PEO homopolymer systems[18] after $AuCl_4^-$ reduction:

$$(AuCl_4^-)-(\text{PEO}-\text{PPO}-\text{PEO})_n \rightarrow \text{Au} + 4Cl^- + 2H^+ + \text{oxidation products} \quad (2)$$

Step 2: Absorption of Block Copolymer on the Surface of Clusters and Reduction of Metal Ions in That Vicinity. Following the formation of gold clusters through reduction of $AuCl_4^-$ ions in solution, block copolymers adsorb on the surface of gold clusters, Au_m, due to the amphiphilic character of the PEO−PPO−PEO block copolymers:[1]

$$Au_m + l\text{PEO}-\text{PPO}-\text{PEO} \rightarrow Au_m-(\text{PEO}-\text{PPO}-\text{PEO})_l \quad (3)$$

where $Au_m-(PEO-PPO-PEO)_l$ represents a gold cluster with adsorbed block copolymers. The adsorbed block copolymers can form pseudo-crown ether structures that bind with $AuCl_4^-$ ions, $Au_m-(PEO-PPO-PEO)_l-(AuCl_4^-)$, and facilitate their reduction.

Step 3: Growth of Metal Particles and Colloidal Stabilization by Block Copolymers. The reduction of $AuCl_4^-$ ions and formation of gold clusters (step 2) is repeated on the surface of gold nanoparticles, and therefore the particles grow.

On the basis of the mechanism proposed above, the kinetics of $AuCl_4^-$ reduction are discussed below in order to examine reactions 1 and 2 in step 1. Reaction 1 is considered the kinetically dominant process in the initial stage of $AuCl_4^-$ reduction so that the reduction rate of $AuCl_4^-$ is given by

$$-\frac{d[AuCl_4^-]}{dt} = k[AuCl_4^-][PEO-PPO-PEO]^n \quad (4)$$

$$[AuCl_4^-] = [AuCl_4^-]_0 \exp\{-k[PEO-PPO-PEO]^n t\} \quad (5)$$

where $[AuCl_4^-]$ is the $AuCl_4^-$ concentration and [PEO−PPO−PEO] is the block copolymer concentration participating in the reaction. $[AuCl_4^-]_0$ is the initial concentration of $AuCl_4^-$, and k is the reduction rate constant. The time evolution of the $AuCl_4^-$ concentration is given by

$$[AuCl_4^-] = [AuCl_4^-]_0 \exp(-Kt) \quad (6)$$

$$K = k[PEO-PPO-PEO]^n \quad (7)$$

where K denotes the apparent rate constant of the reduction. [PEO−PPO−PEO] is assumed to be proportional to the total block copolymer concentration, $[PEO-PPO-PEO]_0$ ($[PEO-PPO-PEO] = k'[PEO-PPO-PEO]_0$), and to be significant smaller than $[PEO-PPO-PEO]_0$. Then eq 7 turns into eq 8, in which K is expressed in terms of $[PEO-PPO-PEO]_0$:

$$K = K'[PEO-PPO-PEO]_0^n \quad (8)$$

$$K' = k(k')^n \quad (9)$$

As shown in eq 6, $[AuCl_4^-]$ decreases exponentially with time after mixing. In the initial stage of the reduction, the concentration of gold nanoparticles is significantly small, so that their contribution to the absorption intensity can be disregarded. The above kinetic analysis does not involve effects of reaction products (e.g., oxidation products) since their concentration must be significantly lower than the total block copolymer concentration at the early stage of $AuCl_4^-$ ion reduction.

In the following sections, we will present the results that support the mechanism proposed above.

Reduction of $AuCl_4^-$ Ions and Formation of Gold Nanoparticles. The proposed formation mechanism of gold nanoparticles suggests that an increase in PEO concentration enhances the particle formation because higher polymer concentration induces the formation of cavities bound with $AuCl_4^-$ ions. To examine the block copolymer concentration dependence on $AuCl_4^-$ reduction and gold nanoparticle formation, we recorded absorption spectra at ∼2 h after mixing of the $AuCl_4^-$ solution with an aqueous Pluronic F108 block copolymer solution at different block copolymer concentrations (see Figure 2). The absorption band centered at ∼220 nm for the gold(III) chloride, $AuCl_4^-$,[26] and the band centered at ∼540 nm originating from the surface plasmon of the gold nanoparticles[27,28] were observed. As the concentration of Pluronic F108 increased, the absorption band centered at 220 nm (due to $AuCl_4^-$) decreased in intensity. This decrease coincides with an increase in the surface plasmon band centered at ∼540 nm. This indicates that gold nanoparticles were formed following the reduction of $AuCl_4^-$.

Figure 3 shows that the absorbance at 240 nm decreased gradually with block copolymer concentration up to 0.6∼1.0 mM and then the value decreased abruptly (at higher block copolymer concentrations, the absorbance at 240 nm started increasing because the gold nanoparticles also absorb in this wavelength range). The increase in reduced $AuCl_4^-$ concentration with increasing block copolymer concentration is consistent with the proposed reaction mechanism. A similar trend is observed when the absorbances at ∼540 nm (due to gold nanoparticles) are plotted as a function of block copolymer concentration (see inset of Figure 3).

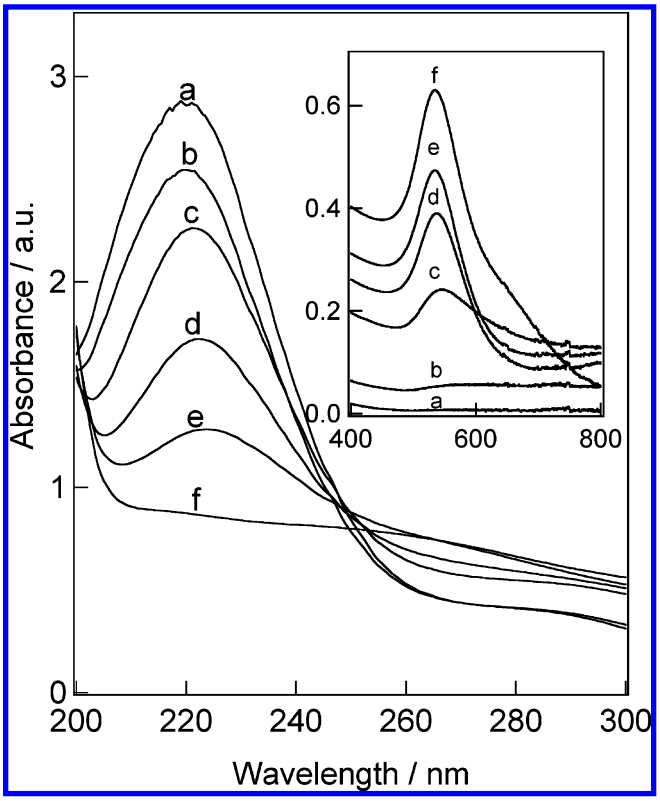

Figure 2. Absorbance spectra centered at ∼220 nm originating from $AuCl_4^-$ ions in Pluronic F108 block copolymer aqueous solutions at different block copolymer concentrations: spectra a−f indicate data at 0.1×10^{-3}, 0.2×10^{-3}, 0.4×10^{-3}, 0.6×10^{-3}, 0.8×10^{-3}, and 1.0×10^{-3} mol L^{-1}, respectively. Inset: Increase in the absorbance spectra centered at ∼540 nm from surface plasmon of gold nanoparticles formed with an increase in Pluronic F108 concentration.

The proposed reaction mechanism also suggests that an increase in PEO chain length (molecular weight) facilitates the reduction of $AuCl_4^-$ and formation of particles.[18−20] PEO−PPO−PEO block copolymers having different PEO block length and similar PPO block length (Pluronic P103, P105, F127 and F108) are compared in Figure 3 at the same block copolymer concentration. The comparison indicates that the absorbance decreased in the order P103 < P105 < F127 < F108, which is in agreement with the order of PEO block molecular weight. This is also consistent with the proposed mechanism.

Also shown in Figure 3, for comparison purposes, are absorbances recorded 2 h after mixing of an aqueous $AuCl_4^-$ ion solution with an aqueous PEO homopolymer solution (the PEO molecular weight was selected to be intermediate among those of Pluronic P103, P105, F127, and F108). At 2 h after the initiation of the reaction, the absorption centered at 240 nm (due to $AuCl_4^-$ ions) was high and independent of PEO homopolymer concentration. The absorbance at ∼540 nm (due to gold nanoparticles) started to increase from ∼0.1 mM Pluronic, while a small increase of absorbance at ∼540 nm was observed after 2 h only above 6.0 mM PEO (see inset of Figure 3). The concentration of reduced $AuCl_4^-$ and gold nanoparticles at 2 h after the reaction initiation in an aqueous PEO homopoly-

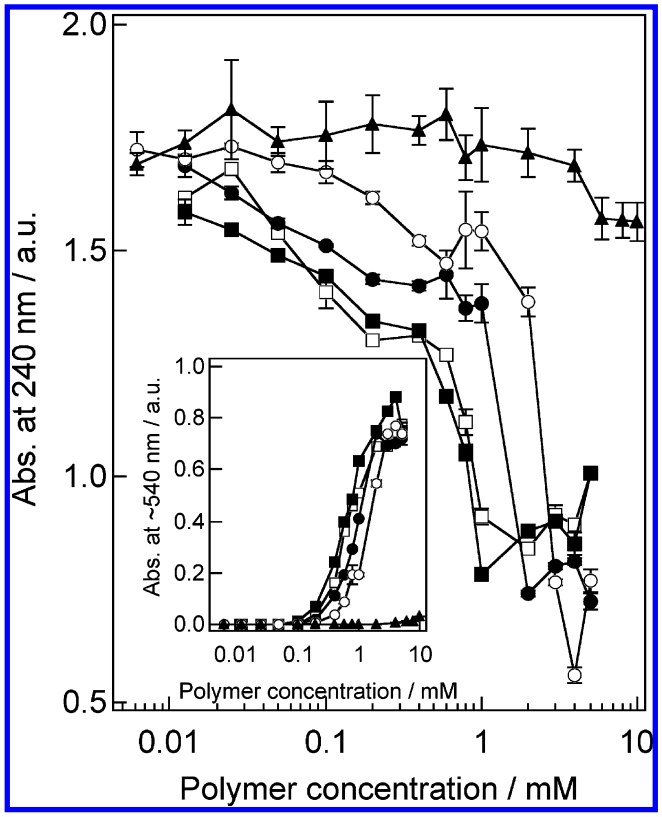

Figure 3. Absorbance at 240 nm recorded at 2 h after mixing of aqueous $AuCl_4^-$ ion solution and aqueous block copolymer P103 (○), P105 (●), F127 (□), and F108 (■) solutions, plotted as a function of polymer concentration. Also shown are absorbances at ~240 nm at 2 h after mixing of aqueous $AuCl_4^-$ ion solutions and aqueous PEO homopolymer solutions (▲). Inset: Absorbances at ~540 nm for the same systems and conditions plotted as a function of polymer concentration.

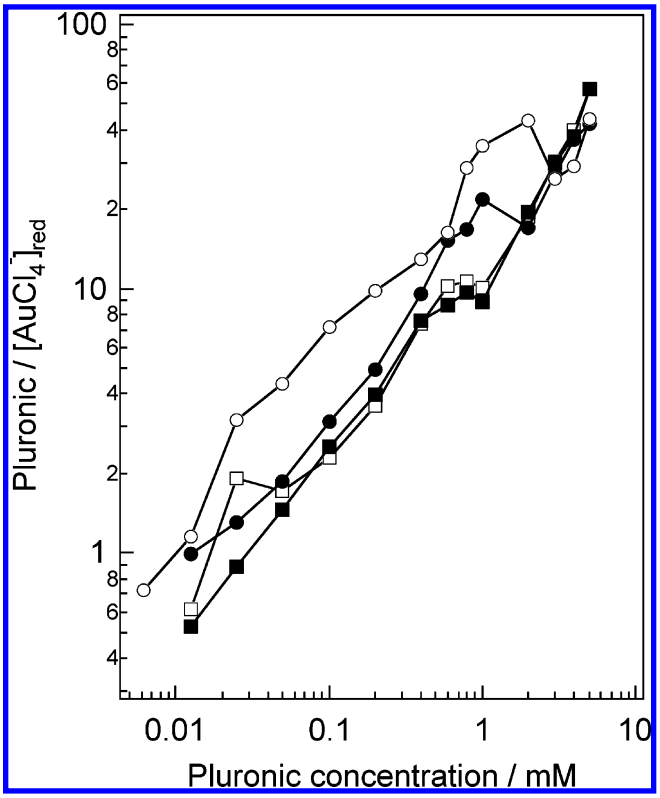

Figure 4. Molar ratio of block copolymer molecules to reduced $AuCl_4^-$ ions, plotted as a function of block copolymer concentration, for Pluronic P103 (○), P105 (●), F127 (□), and F108 (■).

mer solution was much smaller than that in aqueous PEO−PPO−PEO block copolymer solutions even when the molecular weight of the PEO homopolymer is similar to that block copolymer.

Number of Block Copolymer Molecules Reacted per $AuCl_4^-$ Ion. Cavities (pseudo-crown ether structures) can be formed by an individual polymer molecule and also by participation of several polymers.[18,32−38] At a given polymer concentration, longer chain polymers are more active for cavity formation, which is consistent with our results (see Figure 3). An increase in polymer concentration enhances cavity formation by bringing several polymers closer together. An estimation of the number of block copolymer molecules available to react with one $AuCl_4^-$ ion can help us understand the cavity formation component of the reaction mechanism. The Pluronic/$[AuCl_4^-]_{red}$ ratio is plotted in Figure 4 as a function of block copolymer concentration for the same polymers (Pluronic P103, P105, F127, and F108) considered in Figure 3. The reduced $AuCl_4^-$ ion concentration, $[AuCl_4^-]_{red}$, was estimated from the absorption band at 240 nm by use of the extinction coefficient value of 9823 M^{-1} cm^{-1} that has been reported at that wavelength.[26] Figure 4 shows that a larger number of block copolymer molecules is required to reduce one $AuCl_4^-$ ion in the case of shorter block copolymers (lower overall molecular weight or PEO block length). Higher concentration of block copolymer with shorter PEO block length is necessary in order to form cavities, in agreement with the proposed mechanism.

We note that the number of block copolymer molecules reacted with one $AuCl_4^-$ ion is less than 1 at the lower block copolymer range (<0.03 mM) (see Figure 4). This indicates that a single PEO−PPO−PEO block copolymer molecule contains more than 1 reducing equivalent, which is expected given that multiple polymer segments can act as reductants. This high-yield synthesis of gold nanoparticles in PEO−PPO−PEO block copolymer systems reported here is most likely due to high contact probability between block copolymers and $AuCl_4^-$ ions because the pseudo-crown ether conformation of block copolymers binds $AuCl_4^-$ ions.

Contribution of PEO Block to Reduction of $AuCl_4^-$ Ions. PEO blocks contribute to the $AuCl_4^-$ reduction and gold nanoparticle formation as discussed in the previous section (see Figures 3 and 4). The relative contribution of PEO blocks to the $AuCl_4^-$ reduction can be further discerned from the absorbances at 240 nm (due to $AuCl_4^-$) plotted in Figure 5 as a function of (a) molar block copolymer concentration, (b) PEO concentration, (c) PPO concentration, and (d) block copolymer concentration normalized by the block copolymer critical micelle concentration. When plotted as a function of PEO concentration, the data for the different polymers almost overlapped, P103 ≈ P105 ≈ F127 ≈ F108 (see Figure 5b). On the other hand, when the absorbance at 240 nm was plotted as a function of PPO concentration, the absorbance decreased in the order P103 < P105 < F127 < F108 (see Figure 5c). These indicate that the primary contributor to the reduction of $AuCl_4^-$ ions is the PEO concentration (rather than the PPO concentration). The spread of the absorbance data shown in Figure 5d indicates that the presence or not of micelles in the solution does not seem to affect the reduction of $AuCl_4^-$ ions. For example, while the micelle concentration of Pluronic P103 is higher than that of Pluronic F108 at the same overall block copolymer concentration [because of lower cmc (0.141 mM) for Pluronic P103 than that (3.082 mM) for Pluronic F108], the reactivity of Pluronic P103 was lower than that of Pluronic F108 (see Figures 3 and 5d).

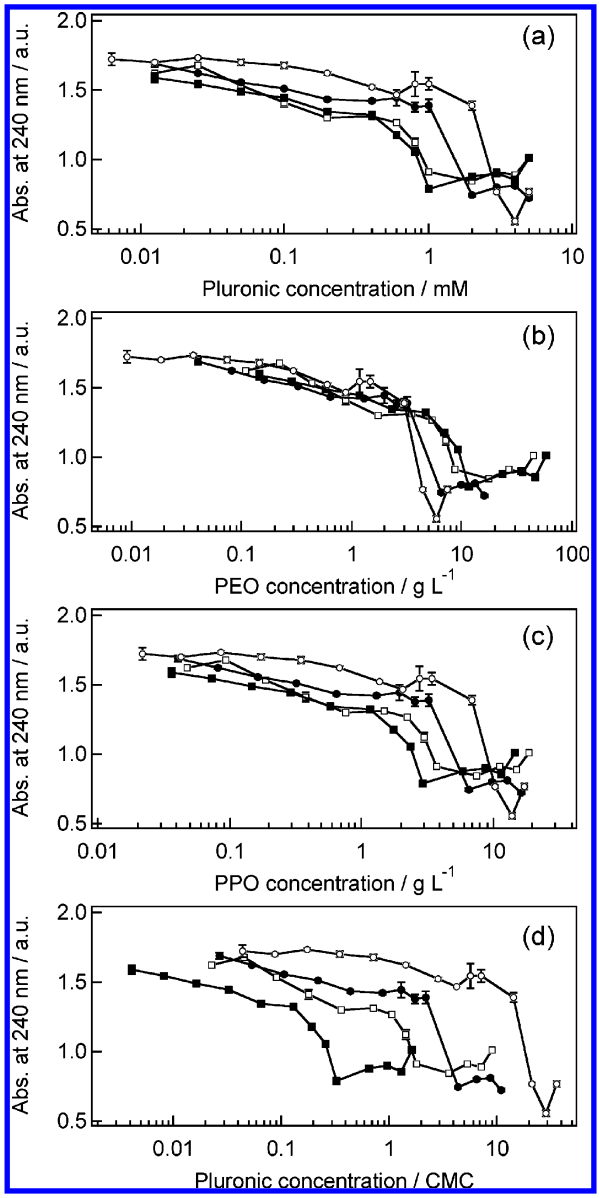

Figure 5. Absorbance changes at 240 nm due to $AuCl_4^-$ ions as a function of Pluronic block copolymer (a) molar concentration, (b) PEO (w/v) concentration, (c) PPO (w/v) concentration, and (d) concentration relative to the critical micelle concentration: P103 (○), P105 (●), F127 (□), and F108 (■).

Contribution of PPO Block to Reduction of $AuCl_4^-$ Ions. Having established the contribution of the PEO blocks to the metal ion reduction, we now turn our attention to the contribution of the PPO blocks. To examine the relative contribution of the overall block copolymer molecular weight and PEO and PPO block lengths on the reduction of $AuCl_4^-$ ions and the formation of gold nanoparticles, we present in Figure 6 absorbances at 240 nm and at ~540 nm at 2 h after mixing of aqueous $AuCl_4^-$ solution with aqueous solutions of several PEO−PPO−PEO block copolymers, plotted as a function of the block copolymer molecular weight, number of EO units, and number of PO units.

The various Pluronic block copolymers that we have considered allow us to assess (i) the effect of overall block copolymer molecular weight at a fixed PEO/PPO ratio (L43, P103, and P123, all with 30% PEO; L44, L64, P84, and P104, all with 40% PEO; P65, P85, and P105, all with 50% PEO; and F68, F88, and F108, all with 80% PEO), (ii) the effect of PEO block length at constant PPO block length (L43 and L44,

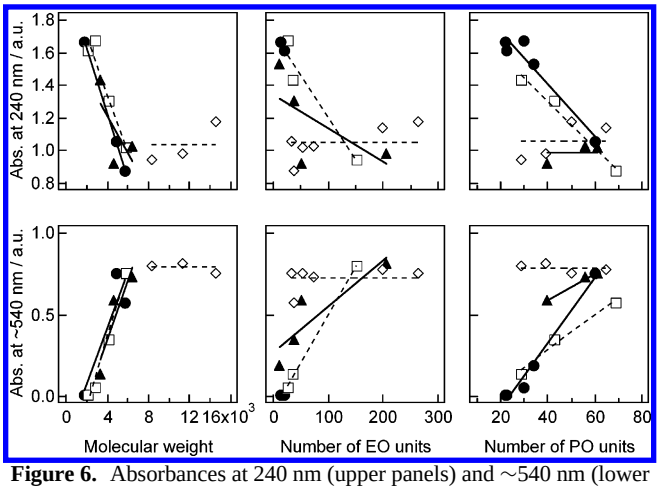

Figure 6. Absorbances at 240 nm (upper panels) and ~540 nm (lower panels) at 2 h after mixing of aqueous $AuCl_4^-$ ion solution and 5.0 mM aqueous PEO−PPO−PEO block copolymer solutions, plotted against the block copolymer molecular weight, number of EO units, and number of PO units. Left-hand side panels: Overall polymer molecular weight at a fixed PEO/PPO ratio [L43, P103, and P123, all with 30% PEO (●); L44, L64, P84, and P104, all with 40% PEO (□); P65, P85, and P105, all with 50% PEO (▲); and F68, F88, and F108, all with 80% PEO (◇)]. Center panels: Effect of PEO block length at constant PPO block length [L43 and L44, both PPO block of ~1300 MW (●); L64, P65, and F68, all having a PPO block of ~1700 MW (□); L62, P84, P85, and F88, all having a PPO block of ~2300 MW (▲); and P103, P104, P105 F108, P123, and F127, all having a PPO block of ~3500 MW (◇)]. Right-hand side panels: Effect of PPO block length [L43, L44, L62, L64, and P103, all with PEO block of <1500 MW (●); P65, P84, and P123, all with PEO block of ~1700 MW (□); P85, P104, and P105, all with PEO block in the range 2000−3000 MW (▲); and F68, F88, F108, and F127, all with PEO block of >6500 MW (◇)]. The open and solid symbols are connected by dashed and solid lines, respectively.

both having a PPO block of ~1300 MW; L64, P65, and F68, all having a PPO block of ~1700 MW; L62, P84, P85, and F88, all having a PPO block of ~2300 MW; and P103, P104, P105, F108, P123, and F127, all having a PPO block of ~3500 MW), and (iii) the effect of PPO block length (L43, L44, L62, L64, and P103, all with PEO block of <1500 MW; P65, P84, and P123, all with PEO block of ~1700 MW; P85, P104, and P105, all with PEO block in the range 2000−3000 MW; and F68, F88, F108, and F127, all with PEO block of >6500 MW). These effects are discussed next.

Effect of Block Copolymer Overall Molecular Weight. As seen from the left-hand side panels in Figure 6, the absorbance at 240 nm (due to reduction) decreased linearly and that at ~540 nm (due to nanoparticle formation) increased with increasing polymer molecular weight for the lower molecular weight range. For block copolymers having higher molecular weight (>8000), the absorbances at 240 nm and at ~540 nm were almost constant. We believe that this is most likely due to the complete reduction of the 0.2 mM $AuCl_4^-$ ions so that absorbances at 240 nm or ~540 nm were saturated at 5.0 mM Pluronic; this can be discerned in Figure 3, where the rate of absorbance change starts to decrease at higher polymer concentration.

Effect of PEO Block Length. The absorbance at 240 nm (due to reduction) decreased linearly and that at ~540 nm (due to nanoparticle formation) increased with increasing PEO block length for block copolymers having shorter PPO block lengths. For block copolymers having PPO block of ~3500 MW, the absorbances at 240 nm and at ~540 nm were almost constant (see center panels in Figure 6), most likely because of complete $AuCl_4^-$ reduction.

Effect of PPO Block Length. As seen in the right-hand side panels in Figure 6, the absorbance at 240 nm decreased linearly

and that at ~540 nm increased with increasing block copolymer PPO length for block copolymers having shorter PEO block lengths. For block copolymers having longer PEO block lengths, the absorbances at 240 nm and at ~540 nm remained almost constant, for the same reason discussed above.

The mechanism presented in the section Proposed Mechanism of Gold Nanoparticle Formation is consistent with the observed increase in reaction activity with increasing molecular weight, PEO block length (see Figures 5 and 6), and/or concentration (see Figure 3) of PEO−PPO−PEO block copolymer. Moreover, our findings indicate that PPO blocks also contribute to the reaction activity (see Figure 6). On the basis of the observed immiscibility between PPO homopolymer and metal ion aqueous solution, it has been suggested[12] that PPO blocks could not directly contribute to the reduction of metal ions. However, results published by our group indicate sufficient hydration of PO segments in aqueous micellar PEO−PPO−PEO block copolymer solutions.[42] Yanagida et al.[33] have found contributions of PPO homopolymer on metal ion complexation (but significantly smaller than that of PEO homopolymer).

The contributions of PPO blocks to $AuCl_4^-$ reduction become more prominent at the later stage of the reaction. For example, $AuCl_4^-$ reduction and gold nanoparticle formation upon reaction completion (~2 h) followed the order P65 < P84 < P123 (data plotted in Figure 6), which is consistent with increasing PPO molecular weight. However, the apparent rate constants at the early stage of $AuCl_4^-$ reduction (as discussed in the following section) increased in the order P65 > P84 > P123 (data plotted in Figure 9), which is the opposite order of PPO molecular weight for these block copolymers having all ~1700 PEO molecular weight.

Early-Time Reduction of $AuCl_4^-$ Ions. As previously discussed, the absorption spectra recorded upon reaction completion showed that PEO−PPO−PEO block copolymers are much more effective than PEO homopolymer in the formation of gold nanoparticles (see Figure 3). Moreover, while the overall block copolymer (i.e., both PEO and PPO blocks) contributes to the formation of gold nanoparticles, the PEO contribution is dominant. So, the question remains why PEO−PPO−PEO block copolymer systems appear more effective than the PEO homopolymer system even when the block copolymer overall molecular weight or the PEO block molecular weight are lower than that of PEO homopolymer. To address this question, we focus on the initial stage of metal ion reduction, which corresponds to step 1 of the proposed mechanism (the absorbance recorded at 2 h after the reaction initiation includes contributions from all the steps, 1−3). In the initial stage of the reduction, the concentration of gold nanoparticles is significantly small, so that the absorption intensity of the gold nanoparticles can be disregarded.

Figure 7 shows the time evolution of [$AuCl_4^-$] following mixing of Pluronic F108 block copolymer solutions with $AuCl_4^-$ solution at different block copolymer concentrations. The reduction proceeded immediately after mixing, and the absorption band of $AuCl_4^-$ decreased with elapsed time. At 5.0 mM block copolymer, [$AuCl_4^-$] seems to increase with elapsed time, but this is because of the overlap with the absorption band originating from the gold nanoparticles. This is the reason we used only short times (40 s) after the reaction was initiated for the analysis of kinetic experiments of $AuCl_4^-$ reduction.

To examine the mechanism of $AuCl_4^-$ reduction by PEO−PPO−PEO block copolymer and PEO homopolymer, we plot the apparent rate constants, *K*, as a function of polymer concentration in Figure 8. *K* was obtained by fitting an exponential function (eq 6) to the changes with time of $AuCl_4^-$ concentration. The apparent rate constant values remained unchanged up to about 0.1 mM block copolymer concentration. Above 0.1 mM block copolymer, *K* increased with increasing block copolymer concentration in Pluronic F127 and F108 solutions but decreased in Pluronic P103 and P105 solutions. Also shown in Figure 8 for comparison purposes are apparent rate constants for the reduction of $AuCl_4^-$ in aqueous PEO homopolymer solutions. *K* decreased slightly with increasing PEO homopolymer concentration.

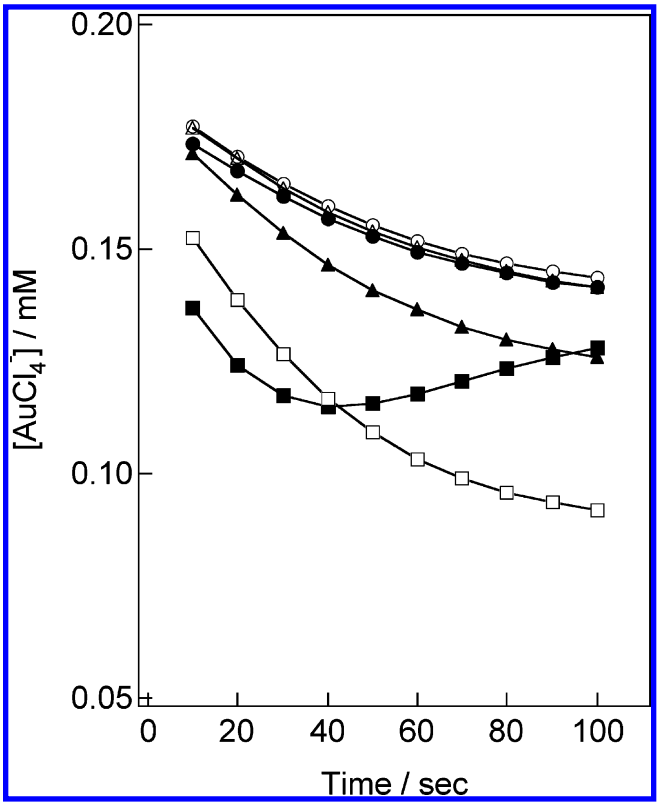

Figure 7. Time evolution of $AuCl_4^-$ concentration following mixing of Pluronic F108 block copolymer solutions with $AuCl_4^-$ solution at different block copolymer concentrations, 0.001 25 (○), 0.05 (●), 0.1 (△), 0.4 (▲), 1.0 (□), and 5.0 mM (■). Measurements started immediately following the initial (10 s) agitation of block copolymer solutions and $AuCl_4^-$ solution.

Comparison of apparent rate constant in these polymers yielded that the apparent rate constant increased in the order P103 < P105 < PEO < F127 < F108, which agrees with the order of increasing PEO block molecular weight. This order is different from that obtained from absorption spectra recorded at 2 h after the reaction was initiated, PEO ≪ P103 < P105 < F127 < F108 (see Figure 3). After 2 h, the concentrations of reduced $AuCl_4^-$ ions and gold nanoparticles formed in the aqueous PEO homopolymer solution were significantly smaller than those in aqueous block copolymer solutions. These findings suggest that the process of $AuCl_4^-$ reduction in block copolymer systems (step 1) is the same as that in the PEO homopolymer system (and is facilitated mainly by the PEO block), while the particle formation (growth) process in PEO−PPO−PEO block copolymer systems (steps 2 and 3) is different from that in the PEO homopolymer system. This can be attributed to the amphiphilic character of PEO−PPO−PEO block copolymers.

Interaction between Block Copolymers and $AuCl_4^-$ Ions. In the kinetics experiments of early time $AuCl_4^-$ reduction, the apparent rate constants, *K*, observed in Pluronic F127 and F108 solutions increased with an increase in the block copolymer

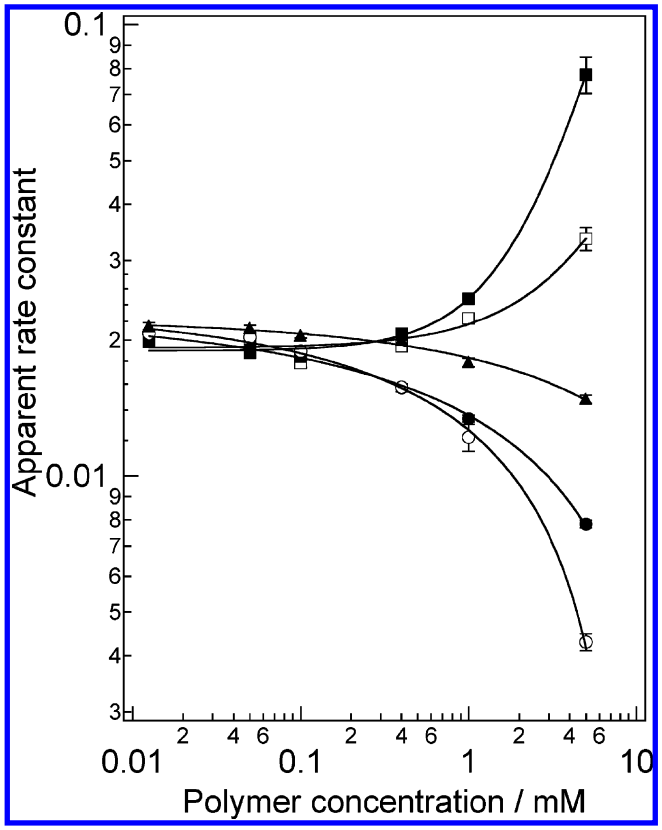

Figure 8. Apparent rate constants *K*, plotted as a function of block copolymer concentration, for P103 (○), P105 (●), F127 (□), and F108 (■). Also shown are apparent constants for PEO homopolymer (▲). The apparent rate constants were obtained from fitting eq 6 to the time course of absorbance changes shown in Figure 7.

concentration above 0.1 mM, while those in Pluronic P103 and P105 solutions decreased with an increase in the block copolymer concentration. This difference can be due to interactions between PEO−PPO−PEO block copolymers and $AuCl_4^-$ ions. To examine this possibility, we obtained the rate constant, K', by fitting the data of Figure 8 to eq 8. $K' > 0$ in the case of Pluronic F127 (0.0025) and F108 (0.0058), while $K' < 0$ in Pluronic P103 (−0.0107) and F105 (−0.0091). Since the rate constant, k, is always positive (because the reaction proceeds forward), k' values must be positive ($k' > 0$) in the case of Pluronic F127 and F108 and negative ($k' < 0$) in Pluronic P103 and F105. Namely, the amount of block copolymer participating in the reaction increases in Pluronic F127 and F108 systems and decreases in Pluronic P103 and F105 systems with increasing total block copolymer concentration.

This difference is most likely due to the level of hydration (swelling) of the PEO−PPO−PEO block copolymers, which is related to their hydrophilic/hydrophobic balance and PEO/PPO ratio. Because of their higher PEO content, Pluronic F127 or F108 is more significantly hydrated than Pluronic P103 or P105. This facilitates contact and reaction with $AuCl_4^-$ ions. In addition, polymer network structures (loops and entanglements) formed in the solution affect the formation of pseudo-crown ether structures and consequently affect the $AuCl_4^-$ reduction rate. It has been reported that looping of a polymer chain enhances the complexation rate of polymers with metal ions but entanglement among different polymer chains does not.[43] Polymer entanglement would increase with increasing polymer concentration, so that the rate constant would tend to decrease with increasing polymer concentration in all systems. Micelles (formed at higher polymer concentrations) could promote polymer entanglements. So the positive K' values in Pluronic F127 and F108 systems are most likely due to the enhancement of looping because of longer polymer chains. The negative K' values in Pluronic P103 and P105 systems are most likely due to difficulty in block copolymer looping because of shorter polymer chains and formation of micelles. The slightly negative K' value (−0.0040) observed for PEO homopolymer solution is most likely due to polymer entanglement. The order of apparent rate constants (P103 < P105 < PEO < F127 < F108) is also consistent with the order of total polymer length (number of segments) [P103(94) < P105(130) < PEO(136) < F127(265) < F108(314)], suggesting that difficulty of polymer looping is related to complexation rate.

To further support this idea, apparent rate constants obtained from 1.0 mM solutions of the block copolymers listed in Table 1 are plotted against the block copolymer overall molecular weight, number of EO units, number of PO units, and cmc in Figure 9. As seen in panels a and b of Figure 9, a minimum point appears. This indicates that an increase of only the overall molecular weight and PEO block length does not always enhance the reduction of $AuCl_4^-$. In the shorter block copolymer or PEO block length range, the apparent rate constant decreased, indicating that $AuCl_4^-$ ions seem to be affected by the hydrophobicity of the block copolymer. Above a certain point, the apparent rate constant increased linearly, indicating that $AuCl_4^-$ ions interact more significantly with block copolymers with longer overall block length or PEO block length because of higher levels of hydration and looping of block copolymers. The correlation between apparent rate constant and PPO block length, explored in panel c of Figure 9, reveals a trend where the apparent rate constant decreases with increasing PPO block length except for block copolymers having longer PEO blocks (F68, F88, F108, and F127, all with PEO block of >6500 MW). This indicates that $AuCl_4^-$ reduction at the early stage is prevented by the hydrophobicity of the block copolymer. The cmc seems to affect the initial reduction of $AuCl_4^-$ ions because a maximum point appears at cmc values of about ∼2.0 mM, as seen in panel d of Figure 9. Since cmc is related to the PEO−PPO−PEO block copolymer molecular weight and PEO/PPO content ratio,[25] the apparent rate constants plotted against cmc are related to those plotted against molecular weight (panel a in Figure 9). The apparent rate constants obtained from block copolymers having higher molecular weight, Pluronic F88, F108, and F127, create the maximum point in panel d (corresponding to the right-side data points in panel a in Figure 9) due to a higher level of hydration and looping of block copolymers. The apparent rate constants obtained from block copolymers having lower molecular weight, Pluronic L64, P65, P84, and P85, fall on the right side of the maximum in panel d (corresponding to the left-side data points in panel a in Figure 9). The apparent rate constants obtained from block copolymers having intermediate molecular weight, Pluronic P103, P104, P105, and P123, are located on the left side of the maximum point. These apparent rate constants located on the left side of the maximum point in panel d in Figure 9 are lower than those obtained from Pluronic L64, P65, P84, and P85, which fall on the right side of the maximum in panel d, suggesting that the contribution of micelles to polymer entanglements prevents $AuCl_4^-$ reduction.

Size Distribution of Gold Nanoparticles Formed in Block Copolymer Solutions. The kinetics experiments provide insight into the mechanism of initial reduction of $AuCl_4^-$ (step 1). To clarify the formation (growth) process (steps 2 and 3), the resulting gold nanoparticles were observed by transmission electron microscopy. The mode of particle growth controls the particle size. The proposed mechanism predicts that the particle

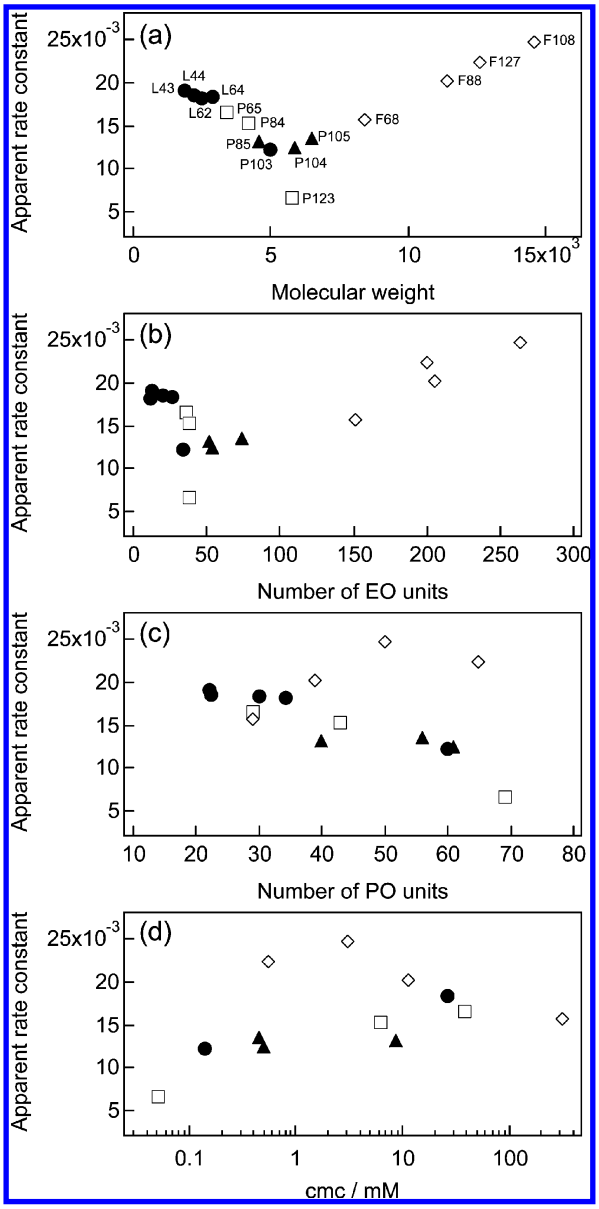

Figure 9. Apparent rate constants *K*, obtained from 1.0 mM solutions of the block copolymers listed in Table 1, plotted against the block copolymer (a) molecular weight, (b) number of EO units, (c) number of PO units, and (d) critical micelle concentration (cmc): L43, L44, L62, L64, and P103, all with PEO block of <1500 MW (●); P65, P84, and P123, all with PEO block of ~1700 MW (□); P85, P104, and P105, all with PEO block in the range 2000−3000 MW (▲); and F68, F88, F108, and F127, all with PEO block of >6500 MW (◇).

size should increase with increasing block copolymer reaction activity, which, in turn, increases with block copolymer concentration or block copolymer length (molecular weight) (see Figure 3).

Figure 10 shows typical transmission electron micrographs of gold nanoparticles obtained in aqueous solutions of Pluronic F108 block copolymer with concentration in the range 0.4−5.0 mM. An increase in the particle average diameter from 6.2 to 20.0 nm was observed with increased Pluronic F108 concentration. Size distributions obtained from electron micrographs of gold nanoparticles produced in Pluronic (a) P103, (b) P105, (c) F127, and (d) F108 block copolymer solutions are shown in Figure 11. In the case of Pluronic P103 and P105 block copolymer solutions, almost monodispersed nanoparticle distributions with diameter below ~20 nm were observed at 0.4 and 1.0 mM block copolymer concentrations, while sizes

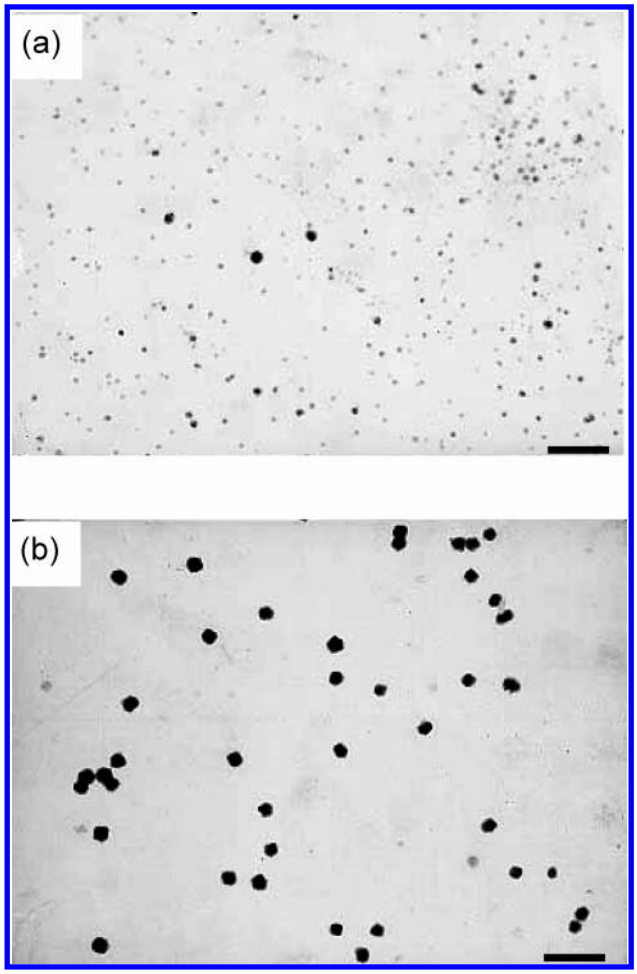

Figure 10. Electron micrographs of gold nanoparticles synthesized in aqueous Pluronic F108 block copolymer solutions with different concentrations: (a) 0.4 and (b) 5.0×10^{-3} mol L^{-1}. The scale bar represents 100 nm.

above 20 nm appeared at 5.0 mM block copolymer (see Figure 11a,b). For Pluronic F127 and F108 block copolymers, almost monodispersed distributions with diameter below ~20 nm were observed at 0.4 mM block copolymer, and sizes above 20 nm appeared at 1.0 mM and 5.0 mM block copolymer (see Figure 11c,d).

The number-average diameters (and standard deviations) of gold nanoparticles produced in Pluronic P103, P105, F127, and F108 solutions increase with block copolymer concentration (as seen in Figure 12a), which is consistent with the corresponding increase in reaction activity. Furthermore, the average diameter seems to increase in the order P103 < P105 < F127 < F108, which is consistent with an increase in reaction activity (or PEO block molecular weight). These results suggest that particle size (growth) was controlled by reaction activity, which is induced by block copolymer length (molecular weight).

Contribution of PPO Block or cmc to Determination of Particle Size. We showed above that the reaction activity enhanced by the block copolymer concentration or PEO block length (overall molecular weight) contributes to the determination of particle size. However, we also have to consider the contributions of PPO block or critical micelle concentration (cmc); in colloidal systems it is common that adsorption process or micelle formation significantly affect the particle size. To examine the contributions of PEO, PPO blocks, and cmc, the number-average diameters of gold nanoparticles produced in Pluronic P103, P105, F108, and F127 solutions are plotted in

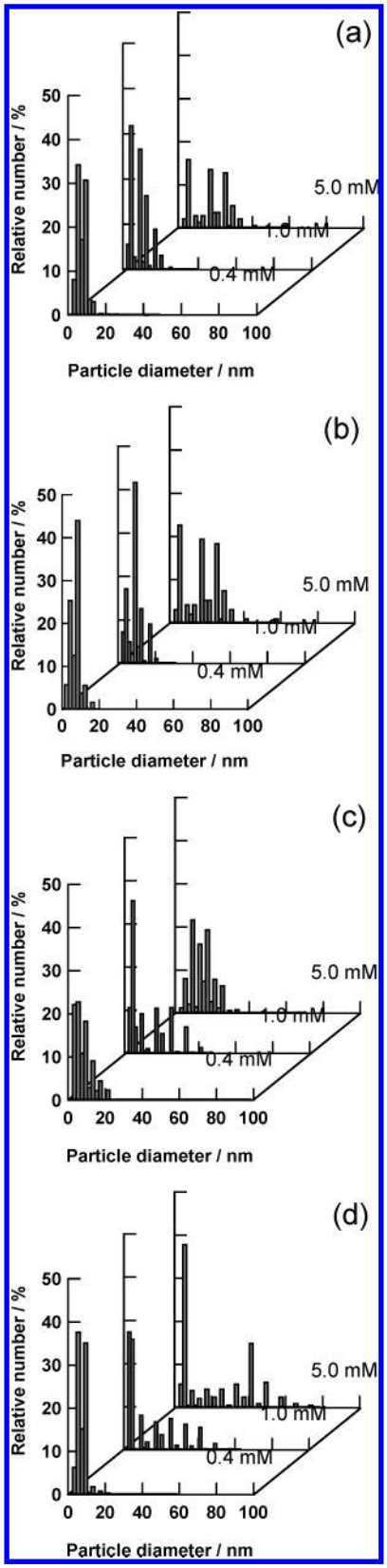

Figure 11. Size distributions obtained from electron micrographs of gold nanoparticles synthesized in aqueous Pluronic (a) P103, (b) P105, (c) F127, and (d) F108 block copolymer solutions.

Figure 12 as a function of (a) block copolymer molar concentration, (b) PEO concentration, (c) PPO concentration, and (d) block copolymer concentration relative to critical micelle concentration (cmc) of Pluronic block copolymers. In the plot of diameter against PEO concentration (see Figure 12b), an

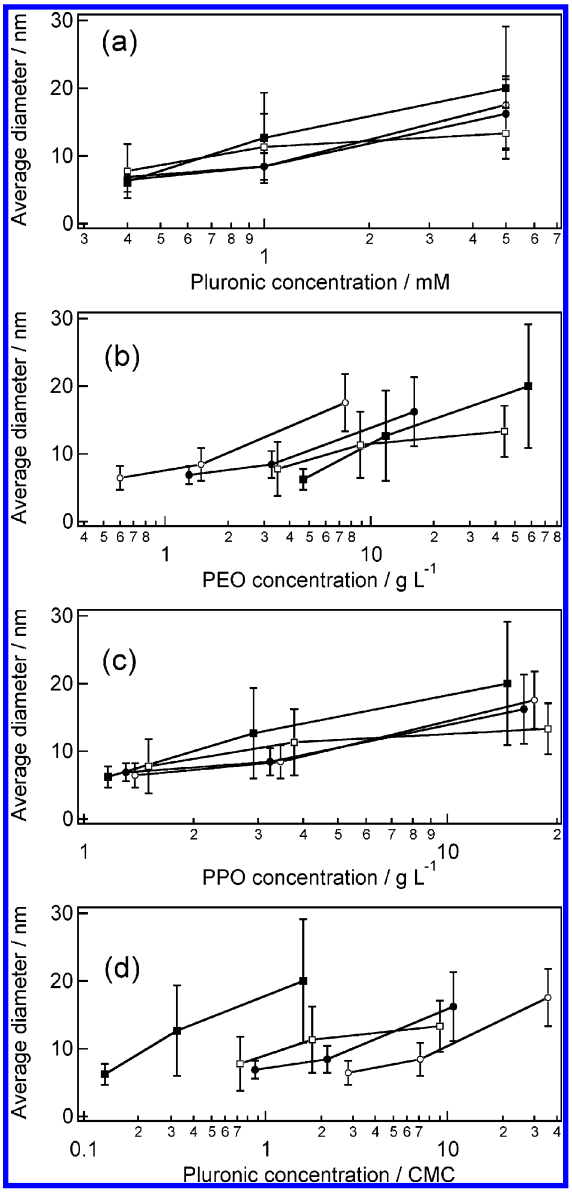

Figure 12. Average diameters of gold nanoparticles produced in aqueous Pluronic block copolymer solutions as a function of (a) molar concentration, (b) PEO (w/v) concentration, (c) PPO (w/v) concentration, and (d) relative concentration to critical micelle concentration of Pluronic block copolymers: P103 (○), P105 (●), F127 (□), and F108 (■). The bars represent 1 standard deviation.

increase in size in the order F108 < F127 < P105 < P103 (at a given PEO concentration) was observed. On the other hand, when plotted against the PPO concentration (see Figure 12b), the diameter values were close to each other for different polymers. This indicates that the PPO concentration also contributes to the particle size determination. When plotted against block copolymer concentration relative to the cmc at 25 °C, the diameter plots were spread in the order of P103 < P105 < F127 < F108 (see Figure 12d). The order of particle size (P103 < P105 < F127 < F108) in Figure 12d is the same below and above the cmc, indicating no major contribution of block copolymer micelles to the particle size determination.

The contribution of PPO concentration to size determination is most likely due to adsorption of PPO blocks on the surface of gold clusters. The adsorption of solutes on the surface of a growing particle is known to limit the particle growth.[44] When PEO−PPO−PEO block copolymers adsorb, PPO blocks prefer to adsorb on the surface due to their hydrophobicity;[1] block

copolymer micelles may attach on the surface of particles above the cmc.[1] If the block copolymer covers the surface of a gold nanoparticle, the effect would be to restrict the final particle size. Namely, competition between (i) reaction activity induced by block copolymer concentration or PEO block length and (ii) block copolymer adsorption induced by PPO block (hydrophobicity) determines the particle size. We believe that the reaction activity due to block copolymer concentration and PEO block length affects the particle growth (size determination) more than the block copolymer adsorption is because the particle size increased with increasing block copolymer concentration and PEO block length when block copolymers with similar PPO molecular weight ~3500 were used (Pluronic P103, P105, F127, and F108).

Conclusions

Poly(ethylene oxide)−poly(propylene oxide)−poly(ethylene oxide) block copolymers proved very efficient in forming nanoparticles from $HAuCl_4$ in aqueous solutions in ambient conditions, in the absence of other reductant and stabilizer. This is due to the amphiphilic character (dual nature) of the PEO−PPO−PEO block copolymers. Formation of gold nanoparticles from $AuCl_4^-$ in aqueous PEO−PPO−PEO block copolymer solutions includes three main steps: (1) reduction of metal ions in aqueous block copolymer solution, (2) absorption of block copolymer on gold clusters because of amphiphilic character (hydrophobicity of PPO) and reduction of further metal ions on the surface of gold clusters, and (3) growth of gold particles and stabilization by block copolymers (refer to Figure 1).

The result from comparison of various PEO−PPO−PEO block copolymers is that the overall block copolymer (i.e., both PEO and PPO blocks) contributes to reduction of $AuCl_4^-$ and particle formation. In the initial reduction process (step 1), PEO is more dominant than PPO. In particular, the level of hydration (swelling) and polymer network structures (e.g., loops and entanglements) of PEO−PPO−PEO block copolymers are related to the initial reduction process (complexation of PEO−PPO−PEO block copolymers with $AuCl_4^-$ ions). PPO would help block copolymer adsorption on gold clusters and the subsequent reduction of $AuCl_4^-$ ions by both PEO and PPO blocks on the surface of the gold clusters (step 2). Thereby the reduction of $AuCl_4^-$ ions would be enhanced on the surface of gold clusters and/or particles (step 3). The higher efficiency of particle formation in block copolymer systems compared to a PEO homopolymer system is caused by the contributions of the adsorption and growth processes (steps 2 and 3). The sizes of gold nanoparticles produced were determined by $AuCl_4^-$ reduction on the surface of gold clusters, which increased with reaction activity of $AuCl_4^-$ reduction induced by the block copolymer overall molecular weight.

Single-step synthesis of metal nanoparticles in aqueous media requires functional polymers or surfactants comprising reduction, adsorption, and stabilization functions. PEO−PPO−PEO block copolymers are nice examples of such molecules. The connection between polymer characteristics and particle formation and size advanced in this study can be useful in elucidating particle synthesis in other polymer media.

The particle formation mechanism by PEO−PPO−PEO block copolymers in aqueous media presents a range of possibilities for further development. The self-assembled structures afforded by amphiphilic polymers[45] can be exploited as nanocontainers, as three-dimensional templates for hybrid metal/polymer ordered materials, and as anchors (when present on surfaces) for surface modification with metal. We are currently exploring interfacial reaction using emulsion systems for synthesis of metal hollow capsules. The tunability of block copolymer self-assembly at oil−water interfaces should be an asset to the above.

Acknowledgment. We are grateful to the National Science Foundation (Grants CTS-0124848/TSE and DMI-0210689/NER) for support of this research.

References and Notes

(1) Lin, Y.; Alexandridis, P. Temperature-Dependent Adsorption of Pluronic F127 Block Copolymers onto Carbon Black Particles Dispersed in Aqueous Media. *J. Phys. Chem. B* **2002**, *106*(42), 10834−10844.

(2) Barnes, T. J.; Prestidge, C. A. PEO−PPO−PEO Block Copolymers at the Emulsion Droplet−Water Interface. *Langmuir* **2000**, *16*(9), 4116−4121.

(3) Yang, L.; Alexandridis, P. Physicochemical Aspects of Drug Delivery and Release from Polymer-Based Colloids. *Curr. Opin. Colloid Interface Sci.* **2000**, *5*, 132−143.

(4) Ivanova, R.; Lindman, B.; Alexandridis, P. Effect of Pharmaceutically Acceptable Glycols on the Stability of the Liquid Crystalline Gels Formed by Poloxamer 407 in Water. *J. Colloid Interface Sci.* **2002**, *252*(1), 226−235.

(5) Kabanov, A. V.; Batrakova, E. V.; Alakhov, V. Y. Pluronic Block Copolymers as Novel Polymer Therapeutics for Drug and Gene Delivery. *J. Controlled Release* **2002**, *82*, 182−212.

(6) Ahmed, F.; Alexandridis, P.; Shankaran, H.; Neelamegham, S. The Ability of Poloxamers to Inhibit Platelet Aggregation Depends on their Physicochemical Properties. *Thromb. Haemostasis* **2001**, *86*(6), 1532−1539.

(7) Cohn, D.; Sosnik, A.; Levy, A. Improved Reverse Thermo-Responsive Polymeric Systems. *Biomaterials* **2003**, *24*(21), 3707−3714.

(8) Soler-Illia, G. J. de A. A.; Crepaldi, E. L.; Grosso, D.; Sanchez, C. Block Copolymer-Templated Mesoporous Oxides. *Curr. Opin. Colloid Interface Sci.* **2003**, *8*(1), 109−126.

(9) Zhao, D.; Feng, J.; Huo, Q.; Melosh, N.; Fredrickson, G. H.; Chmelka, B. F.; Stucky, G. D. Triblock Copolymer Syntheses of Mesoporous Silica with Periodic 50 to 300 Angstrom Pores. *Science* **1998**, *279*(23), 548−552.

(10) Han, Y.-J.; Kim, J. M.; Stucky, G. D. Preparation of Noble Metal Nanowires Using Hexagonal Mesoporous Silica SBA-15. *Chem. Mater.* **2000**, *12*(8), 2068−2069.

(11) Karanikolos, G. N.; Alexandridis, P.; Itskos, G.; Petrou, A.; Mountziaris, T. J. Synthesis and Size Control of Luminescent ZnSe Nanocrystals by a Microemulsion-Gas Contacting Technique. *Langmuir* **2004**, *20*(3), 550−553.

(12) Kim, J.-U.; Cha, S.-H.; Shin, K.; Jho, J. Y.; Lee, J.-C. Preparation of Gold Nanowires and Nanosheets in Bulk Block Copolymer Phases under Mild Conditions. *Adv. Mater.* **2004**, *16*(5), 459−464.

(13) Wang, L.; Chen, X.; Zhan, J.; Sui, Z.; Zhao, J.; Sun, Z. Controllable Morphology Formation of Gold Nano- and Micro-Plates in Amphiphilic Block Copolymer-Based Liquid Crystalline Phase. *Chem. Lett.* **2004**, *33*(6), 720−721.

(14) Alexandridis, P.; Olsson, U.; Lindman, B. A Record Nine Different Phases (Four Cubic, Two Hexagonal, and One Lamellar Lyotropic Liquid Crystalline and Two Micellar Solutions) in a Ternary Isothermal System of an Amphiphilic Block Copolymer and Selective Solvents (Water and Oil). *Langmuir* **1998**, *14*(10), 2627−2638.

(15) Ivanova, R.; Lindman, B.; Alexandridis, P. Evolution in Structural Polymorphism of Pluronic F127 Poly(ethylene oxide)−Poly(propylene oxide) Block Copolymer in Ternary Systems with Water and Pharmaceutically Acceptable Organic Solvents: From "Glycols" to "Oils". *Langmuir* **2000**, *16*(23), 9058−9069.

(16) Sakai, T.; Alexandridis, P. Single-Step Synthesis and Stabilization of Metal Nanoparticles in Aqueous Pluronic Block Copolymer Solutions at Ambient Temperature. *Langmuir* **2004**, *20*(20), 8426−8430.

(17) Sakai, T.; Alexandridis, P. Amphiphilic Block Copolymer Solutions as Media for the Facile Synthesis and Colloidal Stabilization of Metal Nanoparticles. *Polym. Mater. Sci. Eng.* **2004**, *91*, 939−940.

(18) Longenberger, L.; Mills, G. Formation of Metal Particles in Aqueous Solutions by Reactions of Metal Complexes with Polymers. *J. Phys. Chem.* **1995**, *99*(2), 475−478.

(19) Iwamoto, M.; Kuroba, K.; Zaporojtchenko, V.; Hayashi, S.; Faupel, F. Production of Gold Nanoparticles-Polymer Composite by Quite Simple Method. *Eur. Phys. J. D* **2003**, *24*(1−3), 365−367.

(20) Ishii, T.; Otsuka, H.; Kataoka, K.; Nagasaki, Y. Preparation of Functionally PEGylated Gold Nanoparticles with Narrow Distribution through Autoreduction of Auric Cation by α-Biotinyl-PEG-*block*-[poly(2-(*N*,*N*-dimethylamino)ethyl methacrylate)]. *Langmuir* **2004**, *20*(3), 561−564.

(21) Sun, X.; Jiang, X.; Dong, S.; Wang, E. One-Step Synthesis and Size Control of Dendrimer-Protected Gold Nanoparticles: A Heat-Treatment-Based Strategy. *Macromol. Rapid Commun.* **2003**, *24*(17), 1024−1028.

(22) Daniel, M.-C.; Autruc, D. Gold Nanoparticles: Assembly, Supramolecular Chemistry, Quantum-Size-Related Properties, and Applications toward Biology, Catalysis, and Nanotechnology. *Chem. Rev.* **2004**, *104*(1), 293−346.

(23) Pileni, M. P. Metal Particles Made in Various Colloidal Self-Assemblies: Syntheses and Properties. In *Fine Particles: Synthesis, Characterization, and Mechanisms of Growth*; Sugimoto, T., Ed.; Marcel Dekker: New York, 2000.

(24) Bronstein, L.; Antonietti, M.; Valetsky, P. Metal Colloids in Block Copolymer Micelles: Formation and Material Properties. In *Nanoparticles and Nanostructured Films*; Fendler, J. H., Ed.; Wiley-VCH: Weinheim, Germany, 1998.

(25) Alexandridis, P.; Holzwarth, J. F.; Hatton, T. A. Micellization of Poly(ethylene oxide)−Poly(propylene oxide)−Poly(ethylene oxide) Triblock Copolymers in Aqueous Solutions: Thermodynamics of Copolymer Association. *Macromolecules* **1994**, *27*(9), 2414−2425.

(26) Caruso, R. A.; Ashokkumar, M.; Grieser, F. Sonochemical Formation of Gold Sols. *Langmuir* **2002**, *18*(21), 7831−7836.

(27) Link, S.; El-Sayed, M. A. Spectral Properties and Relaxation Dynamics of Surface Plasmon Electronic Oscillations in Gold and Silver Nanodots and Nanorods. *J. Phys. Chem. B* **1999**, *103*(40), 8410−8426.

(28) Link, S.; El-Sayed, M. A. Optical Properties and Ultrafast Dynamics of Metallic Nanocrystals. *Annu. Rev. Phys. Chem.* **2003**, *54*, 331−366.

(29) Barnickel, P.; Wokaun, A. Synthesis of Metal Colloids in Inverse Microemulsions. *Mol. Phys.* **1990**, *69*(1), 1−9.

(30) Liz-Marzan, L. M.; Lado-Tourino, I. Reduction and Stabilization of Silver Nanoparticles in Ethanol by Nonionic Surfactants. *Langmuir* **1996**, *12*(15), 3585−3589.

(31) Chen, D. H.; Huang, Y. W. Spontaneous Formation of Ag Nanoparticles in Dimethylacetamide Solution of Poly(ethylene glycol). *J. Colloid Interface Sci.* **2002**, *255*(2), 299−302.

(32) Liu, K.-J. Nuclear Magnetic Resonance Studies of Polymer Solutions. V. Cooperative Effects in the Ion−Dipole Interaction between Potassium Iodide and Poly(ethylene oxide). *Macromolecules* **1968**, *1*(4), 308−311.

(33) Yanagida, S.; Takahashi, K.; Okahara, M. Metal-Ion Complexation of Noncyclic Polyoxyethylene Derivatives. I. Solvent Extraction of Alkali and Alkaline Earth Metal Thiocyanates and Iodides. *Bull. Chem. Soc. Jpn.* **1977**, *50*(6), 1386−1390.

(34) Warshawsky, A.; Kalir, R.; Deshe, A.; Berkovitz, H.; Patchornik, A. Polymeric Pseudocrown Ethers. 1. Synthesis and Complexation with Transition Metal Anions. *J. Am. Chem. Soc.* **1979**, *101*(15), 4249−4258.

(35) Elliott, B. J.; Scranton, A. B.; Cameron, J. H.; Bowman, C. N. Characterization and Polymerization of Metal Complexes of Poly(ethylene glycol) Diacrylates and the Synthesis of Polymeric Pseudocrown Ethers. *Chem. Mater.* **2000**, *12*(3), 633−642.

(36) Adams, M. D.; Wade, P. W.; Hancock, R. D. Extraction of Aurocyanide Ion-Pairs by Polyoxyethylene Extractants. *Talanta* **1990**, *37* (9), 875−883.

(37) Mathur, A. M.; Scranton, A. B. Synthesis and Ion-Binding Properties of Polymeric Pseudocrown Ethers: A Molecular Dynamics Study. *Sep. Sci. Technol.* **1995**, *30*(7−9), 1071−1086.

(38) Sakai, Y.; Ono, K.; Hidaka, T.; Takagi, M.; Cattrall, R. W. Extraction of Alkali Metal Ions and Tetraalkylammonium Ions with Ionic Surfactants Containing a Polyoxyethylene Chain. *Bull. Chem. Soc. Jpn.* **2000**, *73*(5), 1165−1169.

(39) Yokota, K.; Matsumura, M.; Yamaguchi, K.; Takada, Y. Synthesis of Polymers with Benzo-19-crown-6 Units via Cylcopolymerization of Divinyl Ethers. *Makromol. Chem. Rapid Commun.* **1983**, *4*(11), 721−724.

(40) Ono, K.; Honda, H. Proton NMR Chemical Shift Induced by Ionic Association on a Poly(ethylene oxide) Chain. *Macromolecules* **1992**, *25*(23), 6368−6369.

(41) Beyer, H.; Walter, W. In *Lehrbuch der Organischen Chemie*; Hirzel, 1981.

(42) Yang, L.; Alexandridis, P.; Steytler, D. C.; Kositza, M. J.; Holzwarth, J. F. Small-Angle Neutron Scattering Investigation of the Temperature-Dependent Aggregation Behavior of the Block Copolymer Pluronic L64 in Aqueous Solution. *Langmuir* **2000**, *16*(23), 8555−8561.

(43) Elliott, B. J.; Willis, W. B.; Bowman, C. N. Polymerization Kinetics of Pseudocrown Ether Network Formation for Facilitated Transport Membranes. *Macromolecules* **1999**, *32*(10), 3201−3208.

(44) Hayes, D.; Meisel, D.; Micic, O. I. Size Control and Properties of Thiol Capped CdS Particles. *Colloids Surf.* **1991**, *55*, 121−136.

(45) Alexandridis, P.; Spontak, R. J. Solvent-Regulated Ordering in Block Copolymers. *Curr. Opin. Colloid Interface Sci.* **1999**, *4*, 130−139.